Journal of Physics: Conference Series **500** (2014) 032018 doi:10.1088/1742-6596/500/3/032018

Sound speed measurements in tantalum using the front surface impact technique

P A Rigg, R J Scharff and R S Hixson

Los Alamos National Laboratory, Los Alamos, NM 87545, USA

E-mail: prigg@lanl.gov

Abstract. Shock compression experiments were performed on tantalum to determine the longitudinal sound speed on the Hugoniot from 36 to 105 GPa. Tantalum samples were impacted directly on to lithium fluoride windows at velocities ranging from 2.5 to 5.0 km/s and the resulting particle velocity profiles at the sample/window interface were recorded using optical velocimetry techniques. The time of arrival of the rarefaction wave from the back surface of the tantalum sample was then used to determine the longitudinal sound speed at the corresponding impact stress. In contrast to recently reported work, we see no evidence of a phase transition in the tantalum in this stress range.

1. Introduction

Recent work has suggested that prior to melt, many metals likely go through a solid-solid phase transformation. For example, Burakovsky *et al.* [1] have suggested that tantalum will transform from the bcc phase to the hex-ω phase at ∼100 GPa. This conclusion was based on both the authors' *ab initio* study and the complete body of Hugoniot sound speed data on Ta available in the literature at the time [2–4] plus one previously unpublished data point from the authors of [2]. However, Yao and Klug found the hex-ω phase of Ta to be mechanically and dynamically unstable when anharmonic effects are characterized by high-temperature, self-consistent phonon calculations [5]. More recently, experimental work by Hu *et al.* [6] have suggested that a shock-induced solid-solid phase transition occurs in tantalum at ∼60 GPa based on the results of their Hugoniot sound speed measurements. To further corroborate the existence of a shock-induced solid-solid phase transformation in tantalum, Hsiung and Lassila [7] showed evidence of retained hex-ω phase in recovered Ta samples shocked to 45 GPa.

Key evidence for the existence of this phase transition, however, is missing. Many materials have shown evidence of shock induced solid-solid phase transitions via kinks (discontinuities) in the U_S–u_p curves such as those reproduced in [8] for iron, tin, titanium, and zirconium. In contrast, the U_S–u_p curve for tantalum has been shown to be very linear by several authors [9–12]. Furthermore, Cynn and Yoo [13] have reported the stability of the bcc phase in Ta up to 174 GPa using x-ray diffraction in diamond anvil cell (DAC) experiments. The linearity of the Hugoniot data does not, of course, preclude the existence of a phase transition as the data is linear well into melt [9–12], nor does the absence of a phase transition on the room temperature isotherm from Cynn and Yoo mean that one cannot exist on the Hugoniot. Previous work on molybdenum showed an anomaly in the sound speed data on the Hugoniot at 210 GPa [14] that was attributed to a solid-solid phase transition while the U_S–u_p data [15] was essentially linear.

In light of this well documented controversy surrounding the phase diagram of Ta, we have performed a series of experiments similar to those performed by Hu *et al.* [6] using the front surface impact (FSI or reverse-impact) technique proposed by Duffy and Arhens [16]. Duffy outlined the importance of including the effects of the elastic precursor on the calculation of sound speed in this geometry when two waves are present in the impactor. However, determination of the properties of the elastic state of the material on the Hugoniot (i.e. the Hugoniot Elastic Limit, or HEL) cannot be determined directly in a FSI experiment since (barring kinetic effects) the impactor/window interface reaches the peak state instantaneously at impact. Therefore, the HEL must be determined by other means. When only a single wave is present, we have found that the sound speed determined from analysis of FSI experiments can be extremely sensitive to the accuracy and precision to which the particle velocity at the impactor/window interface is measured.

2. Experimental method

Tantalum samples were directly impacted onto lithium fluoride (LiF) windows as shown in figure 1 and the particle velocity at the sample/window interface was measured using VISAR (Velocity Interferometer System for Any Reflector) [17] and/or PDV (Photon Doppler Velocimetry) [18]. The samples were accelerated using a two-stage gas gun [19] at Los Alamos National Laboratory to velocities ranging from 2.5 to greater than 5 km/s and produced stresses from 36 to approximately 105 GPa. A thin coating (∼400 nm) of aluminum was vapor deposited on the impact surface of the LiF window to obtain a reflective surface for the velocimetry measurements. Previous studies using the FSI geometry have used a buffer [16] or foil [6] glued onto the impact side of the window to preserve the integrity of the reflective surface of the window. However, this can introduce unwanted effects such as the development of multi-wave structure from the elastic precursor of the buffer material or ring-up of the glue bond between the buffer or foil and window. We found that polishing the impact surface of the tantalum impactor was quite effective in preserving the integrity of the mirror after impact and allowed us to measure the true impact state between the sample and window.

3. Experimental results and discussion

Seven FSI experiments were performed in this study and the wave profiles obtained using VISAR for a representative sample of the total set of experiments are shown in figure 2. The values of particle velocity, u_p, shock velocity, U_S, stress, P, and density, ρ, in the shocked tantalum samples were determined from the impedance matching solution [20] between the window with known Hugoniot and the impactor, which is easily derived from the $P - u_p$ diagram shown

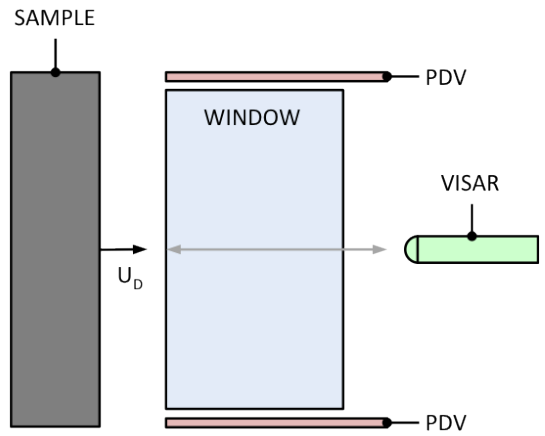

Figure 1. Front Surface Impact (FSI) experimental configuration used to determine the impact state and sound speed in tantalum samples. The impact surface is coated with a thin (∼400 nm) layer of aluminum and velocimetry is obtained at the sample/window interface using VISAR and/or PDV (not shown).

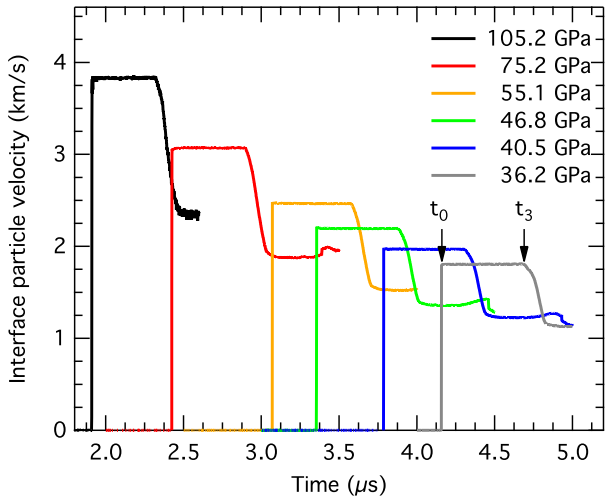

Figure 2. Wave profiles from selected experiments on tantalum. The longitudinal sound speed for each experiment is determined using the time of arrival difference between the leading edge of the rarefaction wave (t_3) and the shock (t_0).

in figure 3(a). The Hugoniot for the window (at rest) is represented by the blue line while the Hugoniot for the impactor traveling to the right (as in figure 1) at a velocity, u_d, is represented by the red line. At impact, both the stress, P^w, and particle velocity, u_p^w, are the same on either side

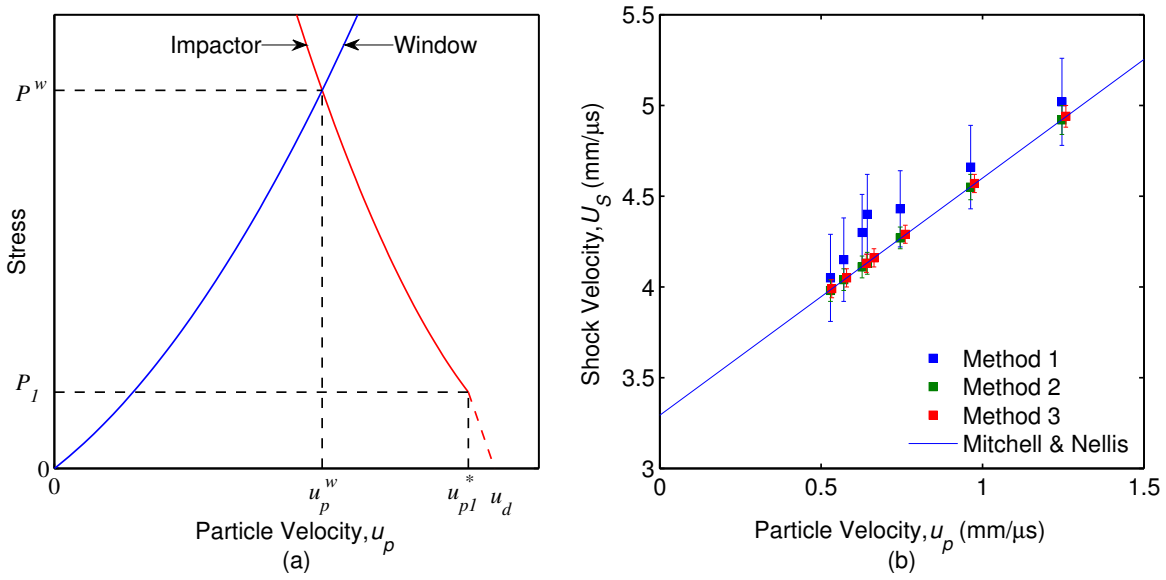

Figure 3. (a) Graphical representation of the impedance matching solution to the Front Surface Impact experiment. The blue line represents the window Hugoniot which is at rest before impact. The red line represents the impactor Hugoniot with an initial velocity of u_d. The dashed section represents the Hugoniot below the Hugoniot Elastic Limit (HEL) while the solid section represents the Hugoniot above the HEL which occurs at (u_{p1}, P_1). Note that $u_{p1}^* = u_d - u_{p1}$. (b) Shock velocities from all 7 FSI experiments calculated using three different methods. Methods 1 and 2 use the measured particle velocity, u_p^w along with the known window or impactor Hugoniot, respectively, to determine U_S. Method 3 uses the known Hugoniots to calculate both u_p^w and U_S.

of the sample/window interface. Thus, given the measured value of u_p^w using VISAR or PDV, the stress at the impactor/window interface is obtained directly from the LiF Hugoniot [21]:

$$P^w = \rho_0^w (C^w + S^w u_p^w) u_p^w, \tag{1}$$

where $\rho_0^w = 2.64 \pm 0.002$ g/cm^3, $C^w = 5.148 \pm 0.054$ km/s, and $S^w = 1.353 \pm 0.022$. The error for C^w and S^w are two sigma values determined with a linear regression of Carter's [21] $U_S - u_p$ data.

As can be seen from figure 3(a), the particle velocity in the impactor is simply given by

$$u_p^i = u_d - u_p^w \tag{2}$$

The stress in the impactor above the the HEL (the solid red curve in figure 3(a)) is represented by the following expression in Lagrangian coordinates:

$$P = P_1 + \rho_0 U_S (u_{p1}^* - u_p), \tag{3}$$

where $u_{p1}^* = u_d - u_{p1}$ and P_1 and u_{p1} are the stress and particle velocity in tantalum at the HEL, respectively. The shock velocity in the impactor was determined using one of three methods. Method 1 used the measured particle velocity at the impactor/window interface and the known window Hugoniot, (1), to solve (3) for U_S at the impact conditions (u_p^w, P^w):

$$U_S = \frac{P^w - P_1}{\rho_0 (u_{p1}^* - u_p^w)}. \tag{4}$$

In Method 2, the measured particle velocity at the impactor/window interface was used in conjunction with the known Hugoniot of the impactor to determine the shock velocity. Here, the particle velocity in the impactor was determined from (2) and we used the tantalum Hugoniot represented by [11]:

$$U_S = 3.293(\pm\ 0.049) + 1.307(\pm\ 0.025)(u_p^i). \tag{5}$$

Finally, Method 3 uses the known Hugoniots of both the window and impactor by combining (1), (2), (3), and (5) at (u_p^w, P^w) to solve for u_p^w and therefore does not use the measured value obtained from velocimetry. This value can then be used in (2) and (5) to find U_S.

In all calculations, we used a single value for the initial density of the tantalum samples of $\rho_0 = 16.68 \pm 0.02$ g/cm^3 as determined from water immersion measurements on several samples. For both Methods 1 and 3, the stress and particle velocity at the HEL are needed to determine the shock velocity. However, these values cannot be determined using the FSI geometry and thus must be determined independently. Furnish *et al.* [22] performed spall experiments on tantalum in which the elastic precursor wave was observed with velocimetry. From these measurements, they were able to derive estimates for the particle velocity, stress, and shock velocity at the HEL. Based on the figures in [22], we estimate that the free surface particle velocity at the HEL is 0.08 ± 0.02 mm/μs. Therefore the in-material particle velocity at the HEL can be estimated as

$$u_{p1} = 0.04 \pm 0.01 \text{ mm}/\mu\text{s}.$$

For the quoted shock velocity value of 4.23 mm/μs, we assume that the actual value cannot be less than the measured longitudinal sound speed. For the samples used here, we determined the longitudinal sound speed ultrasonically to be 4.164 ± 0.009 mm/μs. Thus, we assume that

$$U_{S1} = 4.23 \pm 0.10 \text{ mm}/\mu\text{s}.$$

Then from the jump conditions, $P_1 = \rho_0 U_{S1} u_{p1}$, the stress at the HEL is given as

$$P_1 = 2.8 \pm 0.7 \text{ GPa},$$

where the error was determined using standard propagation of errors. We recognize that these values are estimates only and may even depend on the microstructure of the material. Experiments are currently underway to determine these values more accurately for the material used here.

If the impactor and window Hugoniots and the particle velocity measurements using velocimetry are accurate, all three methods should produce the same results for the shock velocity in the impactor. Figure 3(b) shows the calculated shock velocities in the impactor for all 7 FSI experiments in Eulerian coordinates. The conversion from the Lagrangian to Eulerian frame was done in the usual way:

$$V^E = \frac{\rho_0}{\rho} V^L, \tag{6}$$

where V represents the wave velocity, ρ_0 is the initial density, ρ is the density in front of the wave, and the superscripts, E and L, represent the Eulerian and Lagrangian quantities, respectively. Along with the errors stated in the above discussion, an error of 1% in the measured particle velocity was assumed for all experiments [23] and one sigma error bars on the shock velocity were determined using Monte Carlo error propagation [24]. This figure clearly shows that the three methods do not produce the same values for shock velocity. Methods 2 and 3 are constrained to the Mitchell and Nellis Hugoniot [11] and therefore differ because the calculated particle velocity using Method 3 differs slightly from the measured particle velocity obtained from the VISAR results. The shock velocities calculated using Method 1 have very large error bars and appear to be systematically high when compared to the known Hugoniot. The calculation of shock velocity in this case depends directly on the calculated value of P^w, which itself depends on the square of the measured particle velocity, u_p^w. Not only does this greatly magnify the size of the error bars on the calculated value of U_S, but if the window correction used to determine the actual particle velocity from the measured particle velocity is wrong by even a small amount, then the effect of this on the calculated shock velocity can be large. Changing the particle velocity by only 1% or less is enough to bring all three methods into perfect agreement for the experiments performed here. While the correction factor for LiF determined by Wise and Chhabildas [25] is the generally accepted value (and the one used here), only three experiments were done in that work in the same stress range as the experiments performed here. Thus, it is possible that at these stresses, an error in the window correction – which is the dominant source of error in VISAR measurements [23] – could be contributing to the shift in the data to higher values than expected. It is important to note that the correction factor used here was the power law correction, $\Delta u_p = 0.2784 u_p^{1.031}$ and not the linear correction, $\Delta u_p = 0.281 u_p$ as the linear correction lead to results that were in very poor agreement for the three analysis methods.

Determination of the longitudinal sound speed, C_L, is done with help of figure 4(a) where the times t_0 and t_3 are the arrival times of the shock and rarefaction waves, respectively, as determined from the experimental velocimetry record (see figure 2). This Δt was determined to within a few ns for all experiments. While not observable in the FSI experiment, multiple waves will form in the tantalum impactor until the plastic shock velocity has exceeded the elastic precursor velocity. This "overdriven" condition is illustrated in figure 4(b). Combining (3) (with $P_1 = u_{p1} = 0$) and (5) with a shock velocity of 4.23, this overdriven condition can be expected to occur at stresses above 51 GPa. Therefore, below this stress, the longitudinal sound speed in Lagrangian coordinates is given by,

$$C_L = \frac{h - h_1}{(t_3 - t_0) - \frac{(h-h_1)}{U_S}} \tag{7}$$

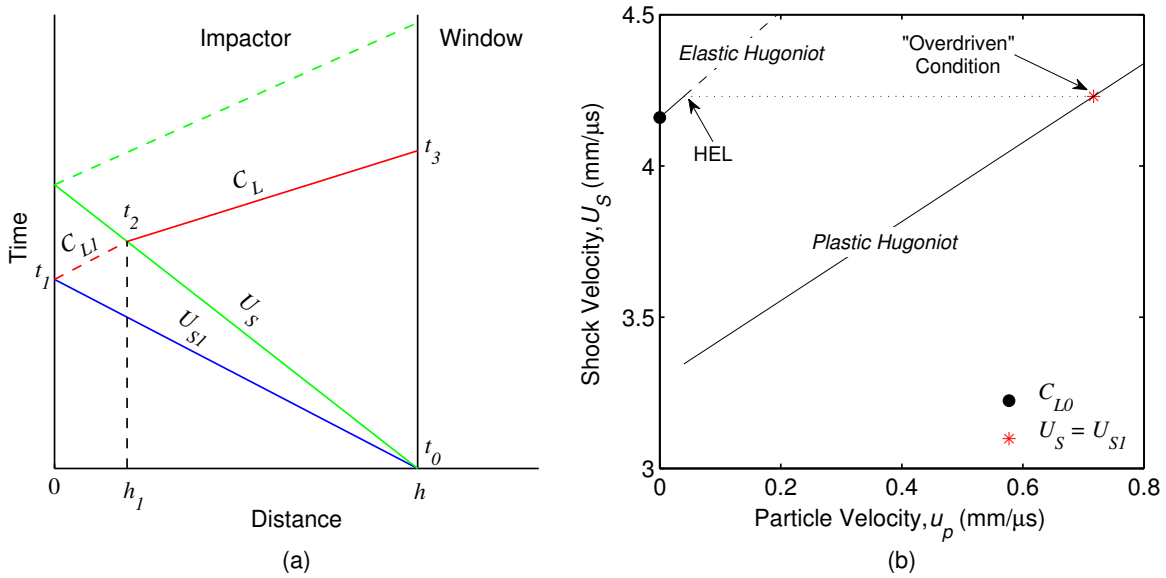

Figure 4. (a) Graphical representation of the propagation of shock and rarefaction waves through the sample. The blue and green solid lines represent the first and second shocks, respectively, while the red line represents the rarefaction traveling through the first (dashed) and second (solid) shocked states. For simplicity, only the leading edge of the rarefaction is shown. (b) Elastic and plastic Hugoniots for tantalum shown in $U_S - u_p$ space. Two-wave structure is observed in shocked tantalum until the plastic shock velocity, U_S is greater than or equal to the elastic shock velocity at the Hugoniot Elastic Limit (HEL), U_{S1}. This is known as the "overdriven" condition. After this condition is met, only a single shock wave is observed.

where

$$h_1 = h\frac{C_{L1}(U_{S1} - U_S)}{U_{S1}(C_{L1} + U_S)} \tag{8}$$

is the transit distance of the rarefaction through the initial state of the material, h is the impactor thickness, U_{S1} and U_S are the shock velocities in the initial and final states, respectively, and C_{L1} is the longitudinal sound speed in the initial state of the material. Above 51 GPa when only a single plastic wave is present, $h_1 \to 0$ in (7).

The results of our analysis of the FSI experiments in figure 2 using (7) and the values of U_S shown in figure 3(b) are plotted in figure 5. The analysis was performed assuming that $C_{L1} = U_{S1} = 4.23$ mm/μs since it was not possible to determine C_{L1} independently. Sound speeds were converted from the Lagrangian to the Eulerian reference frame using (6) and error bars were calculated using the Monte Carlo method [24]. Figure 5(a) shows the results when the linear window correction of Wise and Chhabildas [25] is used while figure 5(b) shows the results when the power law window correction [25] is used to illustrate the importance of determining u_p^w accurately. Reasonably good agreement is seen for the two lowest stress experiments when using the three different methods to calculate the final shock velocity regardless of the window correction used. However, beyond that the points begin to deviate and show different behavior with increasing stress. Sound speeds calculated using Method 1 show a marked decrease in sound speed at approximately 0.6 mm/μs, nearly the same location as the kink reported by Hu *et al.* [6]. In contrast, using Method 2 to determine the sound speed produces a kink in the opposite direction at the same particle velocity while values determined using Method 3 fit nicely to a straight line (solid red lines in figures 5(a) and 5(b)). This demarcation between the three

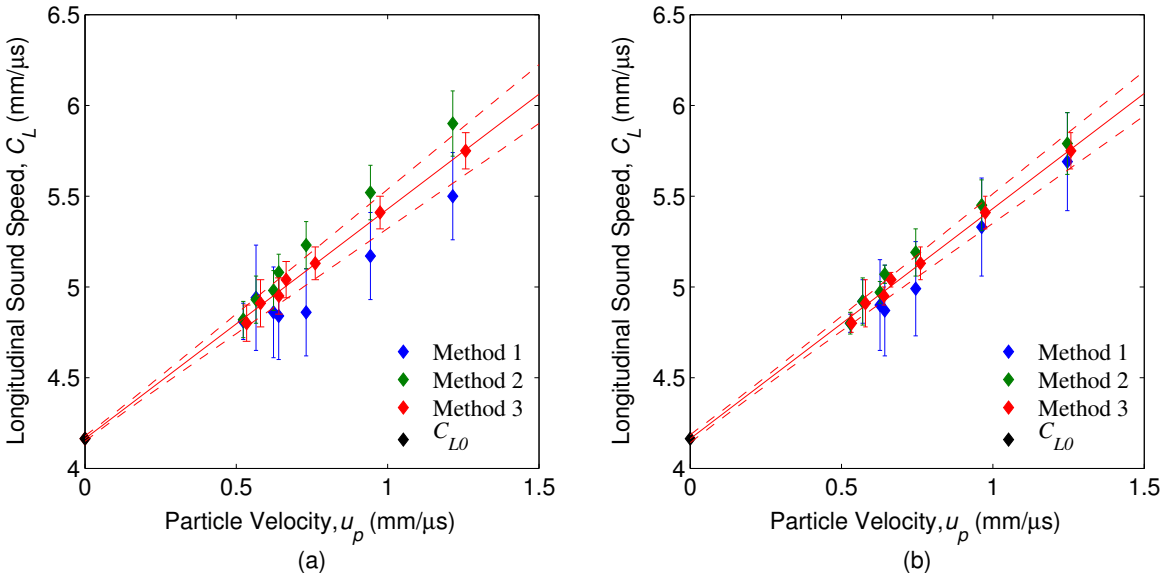

Figure 5. Eulerian longitudinal sound speeds calculated from all 7 FSI experiments using the shock velocities calculated in figure 3(b). In (a), the linear window correction factor of Wise and Chhabildas [25] was used to determine the value of u_p^w used in the Methods 1 and 2 analyses, while (b) shows the results when the power law window correction is used. The red lines represents a linear fit to the "Method 3" results constrained to the ambient longitudinal sound speed, C_{L0}, with 95% confidence bands.

methods is exacerbated when the linear window correction is used (figure 5(a)) and the fact that it is occurring at approximately 50 GPa – the overdrive stress – cannot be a coincidence. In fact, careful examination of figures 3(b) and 4(a) and equation (7) reveal how this can occur. First, below the overdrive stress, the calculation is dominated by the elastic precursor velocity and the dependence on the calculated plastic shock velocity is very small. Above the overdrive stress of course, the calculated plastic shock velocity dominates the calculation of the sound speed. Therefore, the accuracy of the particle velocity measurement when Methods 1 and 2 are used will only affect calculations done above the overdrive stress. Second, regardless of the accuracy of the particle velocity measurement, the *precision* of this measurement has a profound effect on the precision of the calculated sound speed above the overdrive stress, especially when Method 1 is used for the analysis. Here, assuming a precision of $\pm$ 1% in u_p^w produced errors as high as 6% in sound speed. Therefore a premium must be placed on obtaining particle velocity measurements at the impactor/window interface with both high precision *and* accuracy in order to determine useful sound speeds on the Hugoniot when using Methods 1 or 2 to analyze FSI data. In order to reproduce the results obtained using Method 3 with Method 1 requires the particle velocity at the impactor/window interface (and thus the window correction) to be measured to better than 0.1%. While this level of accuracy may not be possible, a refinement of the window correction for LiF is clearly needed and work is now underway to do so.

4. Conclusions

We have performed shock compression experiments on tantalum in the FSI geometry in an attempt to corroborate the existence of a solid-solid phase transition as reported by Hu *et al.* [6]. After carefully considering sources of both random and systematic errors we cannot conclude that a kink in the sound speed is actually being observed in tantalum as the existence

of this kink depends on how the data are analyzed. When the measured particle velocity is used with the window Hugoniot (Method 1) a drop in sound speed is observed. When the measured particle velocity is used with the impactor Hugoniot (Method 2), a rise in the sound speed is observed. Using both the impactor and window Hugoniot to *calculate* the particle velocity (Method 3) produces no kink in the sound speed data. Furthermore, the kink obtained using Methods 1 and 2 occurs when the transition from two-wave to single-wave propagation occurs in the tantalum and corresponds to a change in the dominant variable in this calculation: U_{S1} below and U_S above the overdriven condition. We have demonstrated the profound effect that accuracy and precision of the particle velocity measurement at the impactor/window interface can have on the calculated sound speed when Method 1 is used and recommend that these factors be considered carefully before using FSI experiments to determine sound speed on the Hugoniot. In contrast, if the Hugoniots for the impactor and window are well known, Method 3 should produce accurate results. The values obtained using this analysis method do not show a kink in the sound speed data and therefore we conclude that there exists no evidence in these data to support the existence of a solid-solid phase transition in shocked Ta at stresses below 105 GPa. However, independent verification of these results with careful measurements of the elastic precursor state and sound speeds measured using the overtake method [26] (currently underway) are needed to definitively resolve this controversy.

Acknowledgments

We would like to thank M. E. Byers and S. DiMarino for assistance with the experiments.

References

[1] Burakovsky L, Chen S, Preston D, Belonoshko A, Rosengren A, Mikhaylushkin A, Simak S and Moriarty J 2012 *Phys. Rev. Lett.* **104** 255702
[2] Brown J and Shaner J 1984 *Shock Waves in Condensed Matter – 1983* ed Asay J, Graham R and Straub G (Amsterdam: North-Holland) pp 91–4
[3] Asay J, Chhabildas L, Kerley G and Trucano T 1986 *Shock Waves in Condensed Matter – 1985* ed Gupta Y (New York: Plenum) pp 145–9
[4] Yu Y, Tan H, Hu J, Dai C and Chen D 2006 *Explosion and Shock Waves* **26** 486
[5] Yao Y and Klug D D 2013 *Phys. Rev. B* **88**(5) 054102
[6] Hu J, Dai C, Yu Y, Liu Z, Tan Y, Zhou X, Tan H, Cai L and Wu Q 2012 *J. Appl. Phys.* **111** 033511
[7] Hsiung L and Lassila D 2000 *Acta Mater.* **48** 4851–65
[8] Marsh S P (ed) 1980 *LASL Shock Hugoniot Data* (Berkely: University of California Press)
[9] McQueen R G, Marsh S P, Taylor J W, Fritz J N and Carter W J 1970 *High Velocity Impact Phenomena* ed Kinslow R (New York: Academic Press) pp 343–6, 409–14
[10] Krupnikov K, Bakanova A, Brazhnik M and Trunin R 1963 *Sov. Phys. Dokl.* **8** 205
[11] Mitchell A C and Nellis W J 1981 *J. Appl. Phys.* **52** 3363
[12] Holmes N, Moriarty J, Gathers G and Nellis W 1989 *J. Appl. Phys.* **66** 2962–7
[13] Cynn H and Yoo C S 1999 *Phys. Rev. B* **59** 8526–9
[14] Hixson R S, Boness D A, Shaner J W and Moriarty J A 1989 *Phys. Rev. Lett.* **62**(6) 637–40
[15] Hixson R S and Fritz J N 1992 *J. Appl. Phys.* **71** 1721
[16] Duffy T S and Ahrens T J 1997 *J. Appl. Phys.* **82** 4259–69
[17] Barker L M and Hollenbach R E 1972 *J. Appl. Phys.* **43** 4669–75
[18] Strand O T, Goosman D R, Martinez C, Whitworth T L and Kuhlow W W 2006 *Rev. Sci. Instrum.* **77** 083108
[19] Jones A H, Isbell W M and Maiden C J 1966 *J. Appl. Phys.* **37** 3493–9
[20] Ahrens T J 1987 *Methods of Experimental Physics* vol 24 ed Sammis C G and Henley T L (San Diego, CA: Academic Press) p 185
[21] Carter W J 1973 *High Temp.-High Press.* **5** 313
[22] Furnish M, Chhabildas L, Reinhart W, Trott W and Vogler T 2009 *Int. J.Plasticity* **25** 587–602
[23] Barker L M 1998 *AIP Conf. Proc.* **429** 833–6
[24] Chew G and Walczyk T 2012 *Anal. Bioanal. Chem.* **402** 2463–9
[25] Wise J and Chhabildas L 1986 *Shock Waves in Condensed Matter – 1985* ed Gupta Y (Plenum) pp 441–54
[26] McQueen R G, Hopson J W and Fritz J N 1982 *Rev. Sci. Instrum.* **53(2)** 245